

# Zero-finding methods based on interval arithmetic and their applications to dynamical systems

Nikolay Kryukov<sup>1</sup> and David P. Sanders<sup>1</sup>

<sup>1</sup>*Departamento de Física, Facultad de Ciencias, Universidad Nacional  
Autónoma de México, Ciudad Universitaria, México D.F. 04510, Mexico \**

(Dated: March 15, 2016)

Abstract goes here.

---

\*kryukov@ciencias.unam.mx and dpsanders@ciencias.unam.mx

## I. INTRODUCTION

Chaotic systems form a subset of dynamical systems and are characterized by their high sensitivity to initial conditions. Even though these systems are deterministic (their future behaviour is fully determined by their initial conditions), small differences in initial conditions yield widely diverging outcomes, thus making long-term predictions generally impossible (see, e.g., textbook [1]). Study of chaotic systems has many practical applications in various fields of science, such as physics, engineering, meteorology, biology and economics [2 – 7]. Since chaotic systems are non-integrable, and perturbation methods work only in the cases of small deviations from the integrable system, numerical methods are generally necessary to study such systems.

Methods of computational error control based on order estimates of approximation errors are not rigorous and they do not take into account rounding error accumulation. In this study we use the numerical technique known as interval analysis (IA), interval arithmetic or interval computation. The first books on modern IA were published in 1966 [10, 11]. It has since then been successfully used to solve various problems [12, 13]. The essence of this technique is to compute enclosures (containing intervals) of the values instead of approximations. Simply put, it represents each value as a range of possibilities. Interval algorithms provide rigorous bounds on accumulated rounding errors, approximation errors and propagated uncertainties. Instead of working with a real (uncertain) value  $x$ , we work with the two ends of a closed interval  $[a, b]$  which contains  $x$ . After each operation, the output is an interval which reliably includes the true result [15, 16]. The size of the interval directly gives the rounding error estimate.

In order to develop the software with IA implemented to analyse chaotic systems, we used the programming language Julia [9], developed recently as a high-level open-source dynamic language for scientific and numerical computing with improved performance. Its performance is comparable to or exceeding (2 to 3 times the speed) that of the traditional programming languages like C/C++ due to its sophisticated type system. Using Julia, we created a software package with IA implemented which provides certain computational tools (such as automatic differentiation, interval Newton's method, interval Krawczyk method for one-dimensional and two-dimensional cases) which were applied to chaotic systems studied.

### A. A short overview of interval arithmetic

Despite tremendous increase in the speed and performance of computers in the last decades, not much has changed in the way the actually perform their calculations. Due to the inherent limitations of any finite-state machine, the computations are almost never carried out in a mathematically precise manner. Thus, they do not produce exact results, but rather approximate values that are usually, but not always, near the true ones. To overcome this problem, computational models were developed in which approximate results are automatically provided with guaranteed error bounds. One of these models, interval analysis (IA) was developed by Ramon Moore in the 1960s [10]. We implement this technique following the definitions of W. Tucker [15].

In a nutshell, instead of real numbers, the elements in computations are real intervals (which we denote by bold italic letters)

$$\mathbf{a} = [\underline{a}, \bar{a}] = \{x \in \mathbb{R} : \underline{a} \leq x \leq \bar{a}\} \quad (1)$$

[Further description of IA if needed]

### B. Zero-finding methods

[Chapter in .odt file if needed. Implementation of interval Newton's method and interval Krawczyk method.]

## II. APPLICATION TO A HARD MULTI-DISK SCATTERER IN TWO DIMENSIONS

Using the methods above, we consider the scattering of a point particle in elastic collisions on hard disks fixed in the plane. Such systems have been much studied before because they provide a simple model of chaotic dynamics [ref. Gaspard and others at bottom of p. 176]. We use the Birkhoff mapping [ref. Gaspard or Birkhoff] to output the Birkhoff coordinates  $(\omega, \theta)$  after each collision with a disk:

$$\begin{aligned} \omega_{n+1} &= \omega_n - r_{n,n+1}(\omega_n \cos(\theta_n - \alpha_{n,n+1}) + \sqrt{1 - \omega_n^2} \sin(\theta_n - \alpha_{n,n+1})) \\ \theta_{n+1} &= (\theta_n + \pi + \arcsin \omega_n + \arcsin \omega_{n+1}) \mod 2\pi \end{aligned} \quad (2)$$

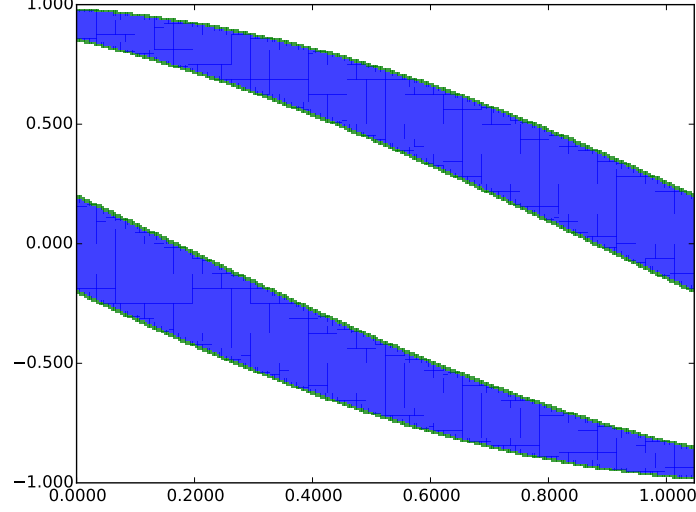


FIG. 1. The cells corresponding to the transition from disk 1 to the other disks in a symmetric 3-disk scatterer, for the tolerance 0.01. The Birkhoff coordinate  $\theta$  is on the abscissa and  $\omega$  is on the ordinate. The rectangles in blue have purity 1 and those in green have purity 0.

where  $\omega_n = \sin \varphi_n$  is the sine of the angle between the incident ray and the normal at the collision,  $\theta_n$  is the angle of the impact point taken anticlockwise with respect to the  $x$ -axis on the  $n$ -th disk,  $r_{n,n+1}$  is the distance between the centers of the  $n$ -th and  $n+1$ -st disk and  $\alpha_{n,n+1}$  is the angle between the vector joining the centers of disk  $n$  to the disk  $n+1$  and the  $x$ -axis.

The Birkhoff mapping contains functions whose domain is not the whole real line. If the input interval causes any of such functions to assume as an argument an interval which does not fully belong to its domain, an exception will be thrown during evaluation. One of the solutions to this problem is so-called decorated intervals [ref.]. A decoration is data attached to the interval to report information, not about the interval as such, but about the process of computing it. In our case, the decoration (which we denote as *purity*) assumes the values of 1, 0 and  $-1$ . Given the starting interval with purity 1, if the interval fully belongs to the domain, the evaluation returns the result with purity 1. If the starting interval intersects with the domain, but does not fully belong to it, the function is evaluated on the intersection and returns the result with purity 0. In case of the starting interval being fully outside of the domain, an empty set is returned with purity  $-1$ .

By bisecting the whole phase space and evaluating the Birkhoff function (or its composition with itself in case of many collisions) on each rectangle until the purity of the result for every rectangle evaluated is either 1 or  $-1$ , or until the tolerance is reached, the purity of the result will indicate whether such a transition exists at the point. Using this, we were able to reproduce Gaspard's results (Ch. 5.2, Fig. 5.6) for the cells of the phase space corresponding to the transitions between the different disks in the case of the symmetric 3-disk scatterer. For example, in 1 we can see the cells corresponding to the transitions from the disk 1 to the disks 2 and 3 (the center of disk 1 is at the origin). These cells also can be expressed analytically (Eqs. (5.36) and (5.37) in ref:Gaspard).

We also made the plots for the escape time function for the symmetric 3-disk scatterer with the distance between the disks  $r = 3.5$  starting from the point with the Cartesian coordinates  $x_0 = -10$  and  $y_0$  varying in the interval  $(0, 0.8)$  and the scatterer has the rightmost disk on the  $x$ -axis and its center of symmetry in the origin. By converting the first collision coordinates from Cartesian to Birkhoff coordinates, we built the plot of the escape time versus the starting  $y$ -coordinate, at a different scale of  $y$ . As in [ref:Gaspard] and [ref:Gaspard article], we can observe the fractal structure of the escape time function.

Using our implemented two-dimensional interval Krawczyk method taking into account purity, we can seek periodic orbits in any two-dimensional multi-disk scatterer. Treating the initial position in Birkhoff coordinates as  $\mathbf{b} = (\omega, \theta)$  and the Birkhoff function (2) as  $\mathbf{T}_{nm}(\mathbf{b})$  for the given system of disks giving the transition from disk  $n$  to disk  $m$ , we obtain the equation for a periodic orbit between disks  $c_i$ , where  $i = 1, 2, \dots, k$ :

$$\mathbf{T}_{c_1 c_2} \circ \mathbf{T}_{c_2 c_3} \circ \dots \circ \mathbf{T}_{c_k c_1}(\mathbf{b}) = \mathbf{b} \quad (3)$$

Placing both sides of (3) on one side, we can seek the zeros of the resulting function, which will give us the initial coordinate for the periodic orbit being sought, providing the range of possible initial coordinates as an interval value of  $\mathbf{b}$ . As an example, we performed the calculation of two periodic orbits in a symmetric 3-disk scatterer with  $r = 6$  oriented as shown in Figure 3

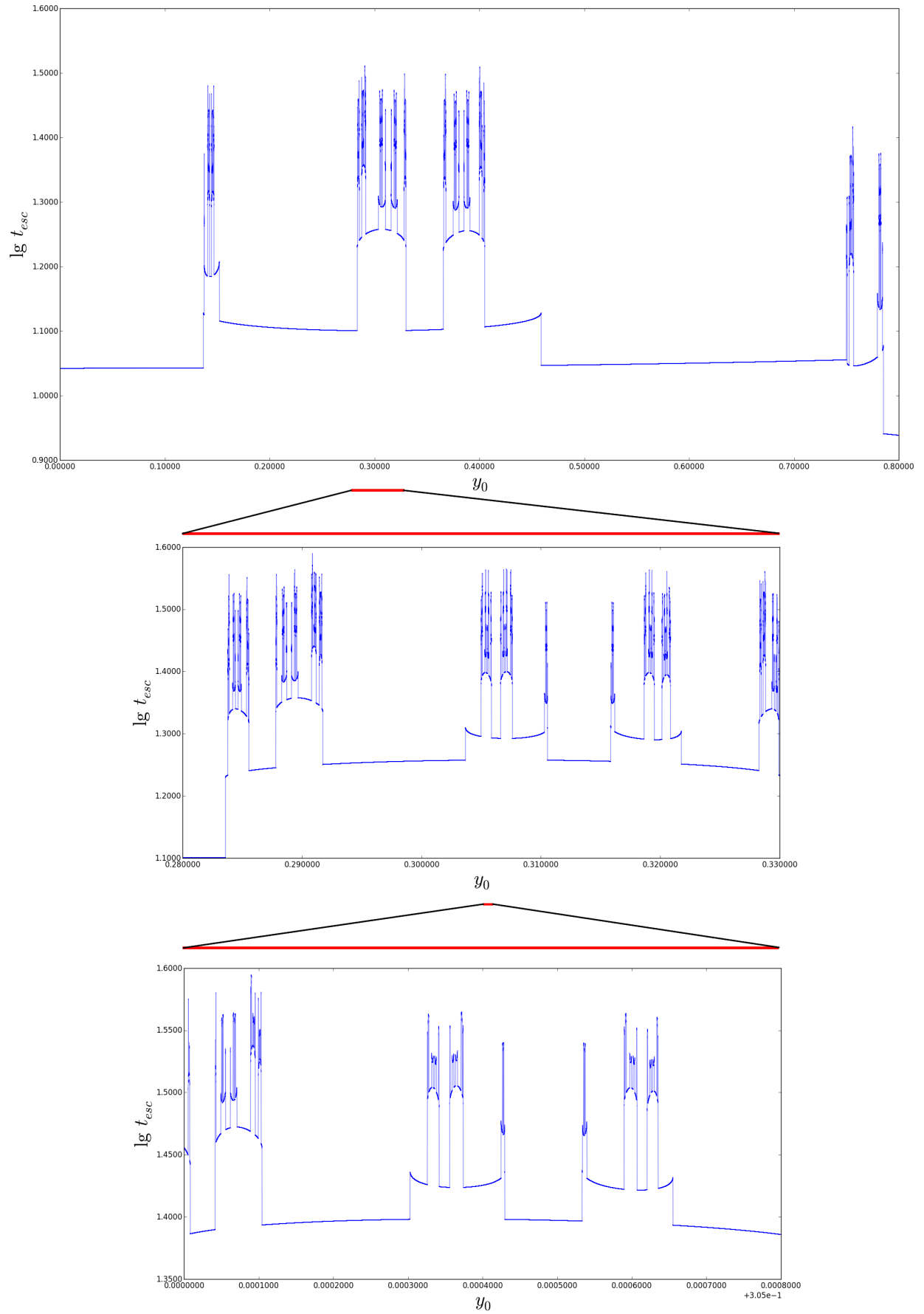


FIG. 2. The escape time function in a symmetric 3-disk scatterer for  $r = 3.5$  and  $x_0 = -10$ , depending on  $y_0$ .

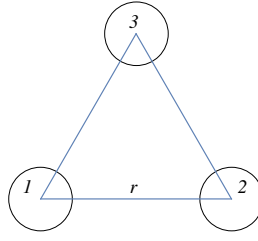


FIG. 3. A symmetric 3-disk scatterer with the origin in the center of disk 1 and the x-axis from the center of disk 1 to that of disk 2.

and also a periodic orbit in a non-symmetric (isosceles) 3-disk scatterer with the disk centers at the coordinates  $(0, 0)$ ,  $(r, 0)$  and  $(r/2, d)$  with  $r = 6$  and  $d = 1.3$  accordingly. The obtained results, together with the analytical results where possible, are given in Tables 1 and 2.

Orbit	Initial Birkhoff point	Initial Birkhoff point (analytical)
123-1	$(-0.\overset{4999999999999999}{5000000000000000}1931, 0.52359877559829\overset{9}{67})$	$(-1/2, \pi/6)$
1213-1	$(-0.581590932\overset{1268368}{2057394}, 0.523598775\overset{6395176}{5570859})$	unknown
123-1 isos.	$(-0.059700088163219\overset{00}{02}, 0.0597356080137144\overset{56}{35})$	$(-\sin \theta_{is}, \theta_{is})$

TABLE I. Initial points in Birkhoff coordinates of some periodic orbits in the symmetric and isosceles 3-disk scatterers.

Orbit	Average length per bounce	Result in [ref:Gaspard]	Analytical result
123-1	$4.267949192\overset{504375}{331957}$	4.2679491924	$r - \sqrt{3}$
1213-1	$4.1582647425\overset{86391}{51725}$	4.1582647426	unknown
123-1 isos.	$2.67862589435\overset{1028}{0730}$	N/A	$\frac{r-2\cos\theta_{is}}{3}(1 + \frac{1}{\cos 2\theta_{is}})$

TABLE II. Average length per bounce of some periodic orbits in the symmetric and isosceles 3-disk scatterers.

In Tables 1 and 2, the value of  $\theta_{is}$  is given by  $\theta_{is} = \arctg p$ , where  $p$  is the minimum positive analytical solution of the equation  $(pr - (d - 1)(1 - p^2))^2 = p^2(1 + p^2)$  with  $r$  and  $d$  being the parameters of the isosceles 3-disk system given above.